Letter

Robust and parallel control of many qubits

Wenjie Gong* and Soonwon Choi
Center for Theoretical Physics, Massachusetts Institute of Technology, Cambridge, Massachusetts 02139, USA

(Received 20 December 2023; revised 15 March 2026; accepted 22 June 2026; published 14 September 2026)

The rapid growth in size of quantum devices demands efficient ways to control them, which is challenging for systems with thousands of qubits or more. Here, we present a simple yet powerful solution: robust, site-dependent control of an arbitrary number of qubits in parallel with only minimal local tunability of the driving field. Inspired by recent experimental advances, we consider access to only one of three constrained local control capabilities: local control of either the phase or amplitude of the beam at each qubit, or individual Z rotations. In each case, we devise parallelizable composite pulse sequences to realize arbitrary single-qubit unitaries robust against quasistatic amplitude and frequency fluctuations. Numerical demonstration shows that our approach outperforms existing sequences such as BB1 and CORPSE in almost all regimes considered, achieving average fidelity >0.999 under a decoherence rate of $\sim 10^{-5}$, even with a few percent amplitude and frequency error. Our results indicate that even for very large qubit ensembles, accurate, individual manipulation can be achieved despite substantial control inhomogeneity.

DOI: 10.1103/n2hz-8zy2

Over the past decade, rapid progress in quantum technology has enabled digital quantum processors to push computational limits [1–4] and analog quantum simulators to unveil insights into diverse many-body phenomena [5–11]. Such investigations involved devices with hundreds of qubits, and it is soon expected that quantum systems with an order of magnitude more qubits will appear [12]. This poses an immediate and pressing challenge: how can we efficiently control a very large number of qubits in realistic settings?

The fast, arbitrary, and robust manipulation of individual qubits within a larger ensemble is difficult in many quantum platforms. In superconducting quantum registers, a considerable number of wires is needed to manage the control and readout of each qubit—a requirement that grows increasingly impractical with larger system sizes [13,14]. Platforms based on quantum optics, including neutral atom tweezer arrays and trapped ions, can partially circumvent this "wire problem" by manipulating qubits with laser beams, thus enabling scalable control through optical technology [15–24].

Though a variety of technical feats, including fast switching rates, high contrast, and low crosstalk, must be achieved to build large-scale systems of optically addressed qubits, multiple array architectures capable of manipulating thousands of different sites have already been demonstrated [25–30]. Nevertheless, implementing high-fidelity, locally controlled unitaries in parallel under realistic conditions remains an outstanding experimental challenge. In particular, in optical platforms, control is accomplished with only a single or few laser beams, making the full individual manipulation of each qubit a complex task to engineer [31,32]. For example, conventional technologies such as acousto-optic deflectors or spatial light modulators are all limited in their degree of local tunability [31].

In this work, we develop a method to efficiently execute robust, arbitrary, site-dependent single-qubit unitaries in parallel for a large number of qubits. Specifically, inspired by recent experimental developments [33–41], we consider three different settings of restricted controls, where one can apply pulses to a qubit ensemble with only minimal local tunability (Fig. 1). Under each such setting, we present the shortest pulse sequences that realize arbitrary single-qubit unitaries in parallel. Furthermore, we devise *parallelizable* composite pulse sequences [42–55] that are robust against both pulse amplitude and off-resonance (detuning) error to account for control imperfections in realistic systems; in large ensembles of qubits, such control errors arise inevitably due to inhomogeneity.

To construct our robust pulse sequences, we combine three key ideas: concatenation, pulse primitives, and numerical search. Concatenation [56] is a technique whereby two pulse sequences that compensate for different errors can be merged to form a doubly robust sequence. Pulse sequences robust against a single type of error—the building blocks of concatenation—are accordingly deemed pulse primitives. We introduce several classes of pulse primitives and, in the absence of an analytical form, further employ gradient-based optimization to numerically search for robust sequences. With these ideas, we create pulse sequences that outperform existing composite pulses, when applicable, at almost any level of amplitude and off-resonance error in the presence of decoherence. Our results thus enable efficient, parallel, and

*Contact author: wgong@mit.edu

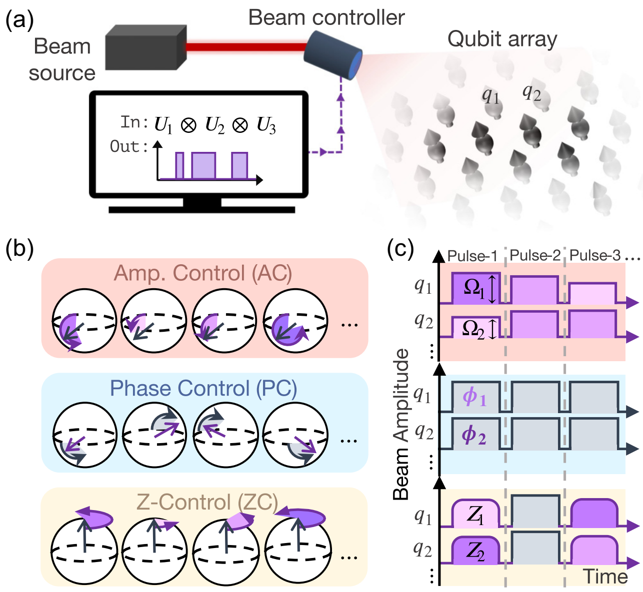

FIG. 1. (a) Many qubits are manipulated in parallel, effecting unitaries $U_1 \otimes U_2 \otimes \cdots$, by applying a sequence of global control beams with restricted tunability. (b) We consider three kinds of local control (purple): the phase (PC) or amplitude (AC) of the beam can be individually controlled, or individual Z rotations can be applied (ZC). (c) Under each type of local control, parallelizable operations are realized by simultaneous pulses on all qubits with a certain locally variable parameter.

high-fidelity quantum information processing on large, near-term quantum systems.

Optimal, parallel, arbitrary unitaries under global driving. Our objective is to realize an arbitrary unitary $\otimes_i U_i$ in parallel across all qubits i under a global driving field, where $\{U_i\} \in$ SU(2) is given as input. In the frame rotating at the frequency of the field, the Hamiltonian of a resonantly driven qubit takes the form $\mathcal{H} = \frac{\Omega}{2}(\cos(\phi)\hat{\sigma}_x + \sin(\phi)\hat{\sigma}_y)$, with Rabi frequency Ω, the phase of the field ϕ, and the Pauli operators $\hat{\sigma}_{x(y)}$. A single pulse of the field is then given by an SU(2) unitary rotation in the x-y plane. We adopt the notation for a pulse $[\theta]_\phi \equiv \exp(-i\frac{\theta}{2}\hat{\sigma}_\phi)$, $\hat{\sigma}_\phi \equiv \cos(\phi)\hat{\sigma}_x + \sin(\phi)\,\hat{\sigma}_y$, which describes a rotation around ϕ in the x-y plane by an angle θ. We further define SU(2) rotations about the axes of the Bloch sphere as $X(\varphi)$, $Y(\varphi)$, and $Z(\varphi)$.

When a global beam is applied to the qubit ensemble, we consider one of three local control capabilities: individual tunability of the phase $\{\phi_i\}$ of the beam (phase control, or PC); individual tunability of the beam intensity $\{\Omega_i\}$ (amplitude control, or AC); or individual rotations about $\hat{z}$ (Z control, or ZC) [Figs. 1(b) and 1(c)]. These schemes are motivated by common experimental approaches; for instance, ZC is enabled by local AC-Stark shifts, a standard practice in trapped-ion systems [33–35], while PC [36,37], AC [36], and ZC [38–41] have also been demonstrated in tweezer arrays.

We now present the optimal sequence to implement $\bigotimes_i U_i$ in each scenario. For AC, as we have site-dependent control of rotation amplitudes, this can be trivially achieved by three pulses:

$$U^{\mathrm{AC}}(\alpha_i, \beta_i, \gamma_i) \equiv [\alpha_i]_0[\beta_i]_{\frac{\pi}{2}}[\gamma_i]_0. \quad (1)$$

The unitary at each qubit i is then parametrized by XYX Euler angles, $U^{\mathrm{AC}}(\alpha_i, \beta_i, \gamma_i) = X(\alpha_i)Y(\beta_i)X(\gamma_i)$, while the phases (rotation axes) are globally fixed. For PC, we can similarly realize

$$U^{\mathrm{PC}}(\alpha_i, \beta_i, \gamma_i) \equiv [\pi/2]_{\alpha_i}[\pi]_{\frac{\gamma_i+\alpha_i-\beta_i}{2}}[\pi/2]_{\gamma_i}, \quad (2)$$

where an explicit calculation shows the equivalence $U^{\mathrm{PC}}(\alpha_i, \beta_i, \gamma_i) = Z(\alpha_i)Y(\beta_i)Z(2\pi - \gamma_i)$, thus capturing all unitaries with ZYZ Euler angles [57]. Finally, the sequence for ZC also follows from ZYZ Euler angles,

$$U^{\mathrm{ZC}}(\alpha_i, \beta_i, \gamma_i) \equiv Z(\alpha_i)[\pi/2]_\pi Z(\beta_i)[\pi/2]_0 Z(\gamma_i), \quad (3)$$

with $U^{\mathrm{ZC}}(\alpha_i, \beta_i, \gamma_i) = Z(\alpha_i)Y(\beta_i)Z(\gamma_i)$. The optimality of these sequences can be shown by simple parameter counting. As an arbitrary unitary requires three parameters and we have one individually tunable variable per pulse, the shortest number of pulses is 3 for AC and PC. For ZC, the three unitary parameters correspond to three individual Z rotations separated by global pulses, leading to an optimal sequence length of 5.

Designing robust pulse sequences. Realistic systems inevitably suffer from various imperfections. When such errors are coherent and quasistatic, or approximately constant, across the duration of a pulse sequence, their effect can be compensated via a cleverly designed "error-correcting" sequence—such a robust sequence is known as a composite pulse. More concretely, suppose that as a result of a small, static error ζ, imperfect rotations $[\theta]^\zeta_\phi = [\theta]_\phi + O(\zeta)$ are implemented. A composite pulse is a sequence of erroneous pulses that together approximate some ideal target unitary $\mathcal{U}$, $[\theta_1]^\zeta_{\phi_1} \cdots [\theta_k]^\zeta_{\phi_k} = \mathcal{U} + O(\zeta^{n+1})$, where the pulse areas $\{\theta_j\}$ and phases $\{\phi_j\}$ are chosen to achieve error cancellation up to order $O(\zeta^n)$. In principle, composite pulses accurate to arbitrarily high order n can be constructed [44,58], with their length k scaling optimally as $k = O(n)$ [58,59]. However, exceedingly lengthy operations are undesirable due to fast time-dependent noise, which leads to decoherence. An inherent trade-off therefore exists between speed and accuracy.

Two prominent sources of coherent, quasistatic error are slow amplitude and frequency drifts of the resonant driving field. Amplitude error, or ϵ error, manifests as a multiplicative error in the pulse area, $\theta \to \theta(1+\epsilon)$, in which $\epsilon = \frac{d\Omega}{\Omega}$, with $d\Omega$ a small error in the Rabi frequency. Off-resonance error, or δ error, leads to a small detuning Δ, which modifies the rotating frame Hamiltonian as $\mathcal{H} = \frac{\Omega}{2}(\hat{\sigma}_\phi + \frac{\Delta}{\Omega}\hat{\sigma}_z)$. Pulses then become $[\theta]^\delta_\phi = \exp(-i\frac{\theta}{2}(\hat{\sigma}_\phi + \delta\hat{\sigma}_z))$, with $\delta = \frac{\Delta}{\Omega}$ the off-resonance fraction. We seek to derive composite pulses for each of the basic sequences [Eqs. (1)–(3)] that compensate for ϵ and δ.

A variety of ϵ- and δ-robust composite pulses already exist, with some of the most celebrated including BB1 [50] and CORPSE [47]. To construct a robust, parallel, arbitrary unitary, we might first attempt to directly replace each of the individual pulses in our optimal solutions with an existing composite pulse. However, this approach of direct replacement encounters two main issues. First, these existing composite pulses are generally not compatible with the constraints imposed by the local control methods considered in this work. Second, the length of such sequences, measured in either the number of pulses k or the total pulse area $T = \sum_j \theta_j$, may be excessive, then increasing vulnerability to other sources of error such as decoherence. In order to address these challenges, we design ϵ-, δ-, and ϵ, δ-robust pulse sequences for each of Eqs. (1)–(3).

Concatenation. Pulse sequences, or primitives, that compensate for either ϵ or δ can be concatenated together to form a sequence simultaneously robust against both errors, as proposed in Ref. [56]. Broadly, concatenation consists of replacing each pulse in an ϵ-robust sequence with a δ-robust composite pulse, or vice versa. However, such a naive substitution can be problematic if the inner composite pulse disturbs the original error-correcting structure of the outer sequence. Thus, a suitable δ-robust inner composite pulse $\mathcal{C}_\delta$ must *preserve* the effect of ϵ, the error it is not designed to correct, a property called *residual error preserving in* ϵ (ϵ-REP) [56]. An overall sequence that compensates to first order in both ϵ and δ can then be obtained by swapping each pulse in an ϵ-robust primitive sequence for a δ-robust *and* ϵ-REP composite pulse. The same holds vice versa in δ and ϵ.

Pulse primitives. With concatenation in mind, we develop appropriate pulse primitives individually robust against ϵ or δ. For first-order δ error compensation, we develop a composite pulse deemed SCORE1 (Switchback for Compensating Off-Resonance Error), whose intuition is given in the Supplemental Material [59]. SCORE1 realizes target rotations $\mathcal{U} = [\theta]_\phi$ and is compatible with all of PC, ZC, and AC, taking the form

$$\mathrm{SCORE1}(\theta, \phi) \equiv [\vartheta_1]_{\phi+\pi}[\theta + 2\vartheta_1]_\phi[\vartheta_1]_{\phi+\pi}, \tag{4}$$

with $\mathrm{SCORE1}(\theta, \phi; \delta) = [\theta]_\phi + O(\delta^2)$ for $\vartheta_1 = \pi - \frac{\theta}{2} - \sin^{-1}(\frac{1}{2}\sin\frac{\theta}{2})$. Generalizations of SCORE1 for higher orders up to $n = 4$ are also listed in the Supplemental Material [59]. Our higher-order SCORE pulse has sequence length that scales linearly with the order of error compensation; to our knowledge, this is the first such δ-robust sequence in the literature and may find use in settings beyond the scope of this article. Our SCORE pulse family is appropriate for concatenation and can directly replace each pulse $[\theta]_\phi$ in the basic sequences [Eqs. (1)–(3)] for parallel, δ-robust arbitrary unitaries.

We turn to ϵ-compensating pulse primitives. Under PC, we insert $[2\pi]_{\phi_j}$ pulses into the sequence we wish to make robust [44,58,60]. Applying this method to Eq. (2) yields a pulse sequence UP1 (Unitaries under Phase control for first-order ϵ compensation),

$$\mathrm{UP1}(\alpha, \beta, \gamma) \equiv [\pi/2]_\alpha[2\pi]_{\phi_1}[\pi]_{\frac{\gamma+\alpha-\beta}{2}}[2\pi]_{\phi_2}[\pi/2]_\gamma, \tag{5}$$

where $\mathrm{UP1}(\alpha, \beta, \gamma; \epsilon) = U^{\mathrm{PC}}(\alpha, \beta, \gamma) + O(\epsilon^2)$ realizes arbitrary SU(2) unitaries for appropriate ϕ_1, ϕ_2. The solution for ϕ_1, ϕ_2, and its higher-order extensions UPn are given in the Supplemental Material [59]. This construction can be understood by noting that in the absence of error, the additional $[2\pi]_{\phi_j}$ rotations will preserve the original sequence. Moreover, when $\epsilon \neq 0$, erroneous $[2\pi]^\epsilon_{\phi_j}$ pulses can be factored as $[2\pi]_{\phi_j}[2\pi\epsilon]_{\phi_j}$; we then use these pure error terms $[2\pi\epsilon]_{\phi_j}$ as a resource to cancel errors in the original sequence through an appropriate choice of ϕ_j.

To develop ϵ-compensating pulse primitives under ZC, we introduce in Theorem 1 a pulse identity allowing us to generate a class of ϵ-robust sequences from a single sequence:

Theorem 1. Under amplitude error in the global drive, a given time-reversal symmetric composite sequence

$$[\theta_1]^\epsilon_{\phi_1}\cdots[\theta_k]^\epsilon_{\phi_k}[\theta_k]^\epsilon_{\phi_k}\cdots[\theta_1]^\epsilon_{\phi_1} = [\theta]_\phi + O(\epsilon^{n+1})$$

implies the class of composite sequences

$$\begin{aligned} Z(\alpha)\,[\theta_1]^\epsilon_{\phi_1}\cdots[\theta_k]^\epsilon_{\phi_k}\,Z(\beta)\,[\theta_k]^\epsilon_{\phi_k}\cdots[\theta_1]^\epsilon_{\phi_1}\,Z(\gamma) \\ = Z(\alpha)\,[\theta/2]_\phi\,Z(\beta)\,[\theta/2]_\phi\,Z(\gamma) + O(\epsilon^{n+1}). \end{aligned}$$

The proof is given in the Supplemental Material [59]. As a consequence of Theorem 1, ϵ-robust sequences for Eq. (3) immediately follow from any time-reversal symmetric composite π pulse.

For AC, we design RA1 (Rotations under Amplitude control for first-order ϵ compensation),

$$\mathrm{RA1}(\theta, \phi) \equiv [\vartheta_1]_{\phi+\frac{\pi}{2}}[\pi]_\phi[2\vartheta_1]_{\phi+\frac{\pi}{2}}[\pi]_\phi[\vartheta_1]_{\phi+\frac{\pi}{2}}[\theta]_\phi. \tag{6}$$

Here, $\mathrm{RA1}(\theta, \phi; \epsilon) = [\theta]_\phi + O(\epsilon^2)$ for $\vartheta_1 = \cos^{-1}(-\frac{\theta}{2\pi})$, implementing arbitrary rotations. To our best knowledge, RA1 is the first ϵ-robust composite pulse that employs global phases and variable pulse areas. The derivation procedure of RA1, as well as a second-order extension of this sequence, is presented in the Supplemental Material [59].

Numerical search. In the absence of any appropriate pulse primitives, we develop a numerical method based on gradient-based optimization to find robust pulse sequences. This numerical search is primarily adapted for AC, in which our individually controllable parameters—the pulse areas—are also subject to error, and the lack of a perfect tuning knob makes robust sequence design more challenging. Specifically, we use gradient ascent to find the pulse areas of a sequence ansatz that maximize fidelity to the target unitary. To ensure robustness, we conduct this maximization over a range of $(\epsilon, \delta, \ldots)$ errors. A detailed explanation of our numerical method is provided in the Supplemental Material [59].

Results. We can now comprehensively state our developed pulse sequences for parallelizable, arbitrary unitaries robust against ϵ, δ, or both under each type of individual control. A concise list of these sequences is provided in Table I; for a graphical schematic of these sequences, see the Supplemental Material [59].

Phase control and amplitude control. Under each of PC and AC, ϵ- or δ-robust unitaries are achieved via our previous pulse primitives. Doubly robust sequences are then obtained by concatenating the two primitives (Table I): for instance, concatenating SCORE1 in UP1 leads to the sequence SCORE1inUP1. For AC, we additionally employ our numerical method to find shorter ϵ-robust and doubly robust sequences [59].

Z control. Unlike PC and AC, ZC assumes the ability to apply local Z rotations, which are generally subject to additional error beyond ϵ and δ. We thus discuss ZC in further detail. Specifically, the form of the local Z error naturally depends on the specific experimental implementation of ZC. In multiple platforms, local $Z(\varphi_i)$ rotations have been realized through AC-Stark shifts induced by a far-detuned field with varying intensity [33,34,40]. Under off-resonant

TABLE I. A summary of pulse sequences introduced in this work. In the ϵ-robust column, the first letter of each sequence indicates either target unitaries or rotations, while the second specifies either PC, ZC, or AC. The number stipulates the order of error compensation. As a general-purpose δ-robust composite pulse, SCORE does not follow this convention.

Control	ϵ robust	δ robust	ϵ, δ robust
PC	UP1	SCORE1[a]	SCORE1inUP1
ZC[b]	UZ1 sUZ1	SCORE1[a]	SCORE1inUZ1
AC	RA1[a] numerical	SCORE1[a]	SCORE1inRA1[a] numerical

[a]Robust unitaries are achieved by directly replacing each pulse in the corresponding basic sequence [Eqs. (1)–(3)] with the robust pulse.
[b]Sequences are presented for $\epsilon_s \ll \epsilon, \delta$. Robust sequences for large ϵ_s are found numerically.

driving at Rabi frequency Ω, qubit evolution in the rotating frame becomes $\exp(-i\mathcal{H}t) = \exp(-i\frac{1}{2}\frac{\Omega^2 t}{2\Delta}\sigma_z) \equiv Z(\varphi)$, with $\varphi = \frac{\Omega^2}{2\Delta}t$. Thus, small drifts in the Rabi frequency $\Omega + d\Omega$ during local gates will lead to a local Stark error (ϵ_s error) $\varphi \to \varphi(1+\epsilon_s)$, $\epsilon_s = 2\frac{d\Omega}{\Omega} + (\frac{d\Omega}{\Omega})^2$, in addition to ϵ and δ error in the global pulses. We therefore address three different regimes: $\epsilon_s \gg \epsilon, \delta$, when local errors dominate; $\epsilon_s \ll \epsilon, \delta$, when global errors dominate; and $\epsilon_s \approx \epsilon, \delta$, when all errors contribute.

When $\epsilon_s \gg \epsilon, \delta$, our global pulses are almost perfect, and we can treat $[\frac{\pi}{2}]_\pi Z(\varphi_i)[\frac{\pi}{2}]_0 = Y(\varphi_i)$, where φ_i may contain ϵ_s error. In this case, ϵ_s compensation then directly maps to ϵ compensation under AC via a rotation of Eq. (3) by $Y(-\frac{\pi}{2})$, and we can obtain ϵ_s-robust pulse sequences using a version of our numerical method. When $\epsilon_s \approx \epsilon, \delta$, solutions robust against ϵ_s, ϵ, and δ can similarly be found numerically [59].

When $\epsilon_s \ll \epsilon, \delta$, our local Z rotations are approximately perfect, and Theorem 1 allows us to immediately construct ϵ-robust pulse primitives for U^{ZC} from any time-reversal symmetric composite π pulse. Based on the composite π pulses $[2\pi]^\epsilon_{\phi_1}[\pi]^\epsilon_0[2\pi]^\epsilon_{\phi_1} = [\pi]_0 + O(\epsilon^2)$ and $[\pi]^\epsilon_{\phi_1}[\pi]^\epsilon_{\phi_2}[\pi]^\epsilon_{\phi_1} = [\pi]_0 + O(\epsilon^2)$, we, respectively, devise two different sequences UZ1 and sUZ1 (unitaries under Z control for first-order ϵ compensation),

$$\mathrm{UZ1} \equiv Z(\alpha)[2\pi]_{\bar{\phi}_1}[\pi/2]_\pi Z(\beta)[\pi/2]_0[2\pi]_{\phi_1} Z(\gamma), \tag{7}$$

$$\mathrm{sUZ1} \equiv Z(\alpha)[\pi]_{\bar{\phi}_1}[\pi/2]_{\bar{\phi}_2} Z(\beta)[\pi/2]_{\phi_2}[\pi]_{\phi_1} Z(\gamma), \tag{8}$$

with $\bar{\phi}_j = \phi_j + \pi$. The second sequence sUZ1 is shorter in total pulse area. $\mathrm{UZ1}(\alpha,\beta,\gamma;\epsilon) = U^{\mathrm{ZC}}(\alpha,\beta,\gamma) + O(\epsilon^2)$ for $\phi_1 = \cos^{-1}(-\frac{1}{4})$ and $\mathrm{sUZ1}(\alpha,\beta,\gamma;\epsilon) = U^{\mathrm{ZC}}(\alpha,\beta,\gamma) + O(\epsilon^2)$ for $(\phi_1,\phi_2) = (\frac{\pi}{3}, \frac{5\pi}{3})$. While sUZ1 is shorter, UZ1 better serves as a sequence for concatenation [59]. Order n extensions of both sequences follow straightforwardly [51,59,61], and solutions for the higher-order versions of UZ1 and sUZ1 up to order $n = 5$ are given in the Supplemental Material [59].

As before, δ-robust unitaries are achieved by directly replacing each $\frac{\pi}{2}$ pulse in Eq. (3) with a SCORE

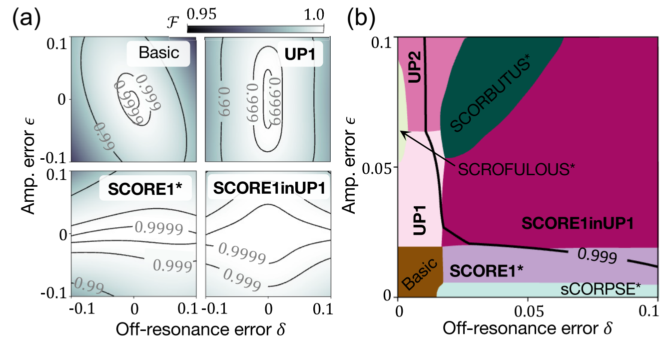

FIG. 2. (a) Fidelity contours at $\gamma = 0$ for our basic sequence in Eq. (2), as well as various parallelizable PC composite pulse sequences averaged over target $\mathcal{U} \in [H, Z(\frac{\pi}{4}), X(\frac{\pi}{2}), Y(\frac{\pi}{2})]$. (b) Phase diagram of the pulse sequence that maximizes $\mathcal{F}$ at each (ϵ, δ) under PC, drawn for $\gamma = 5 \times 10^{-5}\Omega$. Our developed pulse sequences, indicated in bold, occupy most of the parameter range considered here. As γ increases, the basic and first-order sequences will grow to dominate the phase space. See the Supplemental Material [59] for phase diagrams for ZC and AC, as well as for more parameter regimes.

primitive, while double compensating sequences are given by concatenation.

Numerical demonstration. We now numerically test our pulse sequences, benchmarking them against widely adopted existing composite pulses such as BB1 [50] and CORPSE [46]. In practice, various sources of incoherent errors—which cannot be mitigated by composite pulses—also arise over the duration of a pulse sequence and reduce gate fidelity. To capture this effect, we evaluate the average gate fidelity in the presence of decoherence modeled as a depolarizing channel [59]:

$$\mathcal{F} = e^{-\gamma t}\mathbb{E}_\psi\big[|\langle\psi|\mathcal{U}^\dagger\mathcal{U}(\epsilon,\delta)|\psi\rangle|^2\big] + (1 - e^{-\gamma t})/2.$$

Here, $\mathbb{E}_\psi$ denotes averaging over uniformly random initial states, $\mathcal{U}$ is a target unitary, $\mathcal{U}(\epsilon,\delta)$ is a pulse sequence under imperfections, and γ is the decoherence rate.

We compute $\mathcal{F}$ over a wide range of $(\epsilon, \delta, \gamma)$ for both our sequences and other composite pulses, where $\mathcal{F}$ is averaged over the choice $\mathcal{U} \in [H, Z(\frac{\pi}{4}), X(\frac{\pi}{2}), Y(\frac{\pi}{2})]$. Here, H is the Hadamard gate, and $Z(\frac{\pi}{4})$ is the T gate up to a phase. H and T, along with any entangling gate, form a universal gate set. The result is plotted as fidelity contours in ϵ-δ plane, as shown in Fig. 2(a) for our various PC sequences at $\gamma = 0$.

We further construct "phase diagrams" indicating which sequence, among those considered, achieves the highest $\mathcal{F}$ at each point in $(\epsilon, \delta, \gamma)$ phase space. To make these diagrams, $\mathcal{F}$ is averaged fourfold to lie in the positive (ϵ, δ) quadrant. Though each phase diagram depends on the ensemble of target unitaries $\mathcal{U}$, we generically find that our sequences for arbitrary unitaries outperform existing composite pulses almost everywhere in phase space. As an example, we show the phase diagram for PC sequences at $\gamma = 5 \times 10^{-5}\,\Omega$ [Fig. 2(b)], and more extensive numerical results are presented in the Supplemental Material [59]. Figure 2(b) indicates that our PC sequences enable performance at fidelities > 0.999, even in the presence of quasistatic laser amplitude or detuning error up to $\sim$10%.

Discussion. We have developed a method of efficient, parallel, and highly robust control of an arbitrarily large qubit ensemble. Quasistatic errors can be efficiently suppressed by our parallelizable composite pulse sequences, even without knowledge of the precise amount of error present. Consequently, the Rabi frequencies and detunings of individual qubits do not need to be calibrated beyond a percent level in practical situations. Indeed, the simultaneous calibration and removal of spatial inhomogeneity becomes increasingly demanding, or practically infeasible, for larger systems of tens or hundreds of thousands of qubits. Our approach lifts this challenge, having immediate impact for current experiments. Moreover, our method also effectively mitigates other coherent sources of imperfection, such as quasistatic correlated errors.

Although our method may increase vulnerability to incoherent errors such as phase noise and scattering, recent developments indicate that suitably designed qubit encoding and error correction schemes can efficiently contain some decay via conversion into erasure-biased errors [62,63]. Since such error correction techniques may be less effective for coherent control errors [64], the robust control methods presented here complement erasure conversion. When implemented in conjunction, both coherent and incoherent errors can be suppressed in large qubit arrays.

Experimental implementations of our pulses may also benefit from additional closed-loop optimization, perhaps using machine learning [65], to suppress other platform-specific sources of error. Finally, we note that while our work primarily concerns optical controls, a similar approach might also be useful for superconducting qubit systems owing to the reduced number of calibrated operations [57,66].

Acknowledgments. We would like to thank Adam Shaw, Ran Finkelstein, Joonhee Choi, and Manuel Endres for sharing their early experimental results, which inspired this work. We also thank Adam Shaw, Ran Finkelstein, Harry Zhou, Dolev Bluvstein, Marcin Kalinowski, Samuel Li, Sophie Li, Sasha Geim, Manuel Endres, Joonhee Choi, Tracy Northup, and Jeff Thompson for helpful discussion, insights, and providing feedback on earlier version of this article. This work was supported in part by NSF CUA (PHY-1734011), QLCI program (2016245), and CAREER Award (DMR-2237244). W.G. was supported by the Paul and Daisy Soros Fellowship for New Americans and the Hertz Foundation Fellowship.

Data availability. Numerical data is available from the authors upon reasonable request.

[1] F. Arute *et al.*, Quantum supremacy using a programmable superconducting processor, Nature (London) **574**, 505 (2019).

[2] Y. Kim, A. Eddins, S. Anand, K. X. Wei, E. van den Berg, S. Rosenblatt, H. Nayfeh, Y. Wu, M. Zaletel, K. Temme, and A. Kandala, Evidence for the utility of quantum computing before fault tolerance, Nature (London) **618**, 500 (2023).

[3] D. Zhu, G. D. Kahanamoku-Meyer, L. Lewis, C. Noel, O. Katz, B. Harraz, Q. Wang, A. Risinger, L. Feng, D. Biswas, L. Egan, A. Gheorghiu, Y. Nam, T. Vidick, U. Vazirani, N. Y. Yao, M. Cetina, and C. Monroe, Interactive cryptographic proofs of quantumness using mid-circuit measurements, Nat. Phys. **19**, 1725 (2023).

[4] D. Bluvstein, H. Levine, G. Semeghini, T. T. Wang, S. Ebadi, M. Kalinowski, A. Keesling, N. Maskara, H. Pichler, M. Greiner, V. Vuletić, and M. D. Lukin, A quantum processor based on coherent transport of entangled atom arrays, Nature (London) **604**, 451 (2022).

[5] H. Bernien, S. Schwartz, A. Keesling, H. Levine, A. Omran, H. Pichler, S. Choi, A. S. Zibrov, M. Endres, M. Greiner, V. Vuletić, and M. D. Lukin, Probing many-body dynamics on a 51-atom quantum simulator, Nature (London) **551**, 579 (2017).

[6] A. Lukin, M. Rispoli, R. Schittko, M. E. Tai, A. M. Kaufman, S. Choi, V. Khemani, J. Léonard, and M. Greiner, Probing entanglement in a many-body–localized system, Science **364**, 256 (2019).

[7] G. Semeghini, H. Levine, A. Keesling, S. Ebadi, T. T. Wang, D. Bluvstein, R. Verresen, H. Pichler, M. Kalinowski, R. Samajdar, A. Omran, S. Sachdev, A. Vishwanath, M. Greiner, V. Vuletić, and M. D. Lukin, Probing topological spin liquids on a programmable quantum simulator, Science **374**, 1242 (2021).

[8] J. Choi, A. L. Shaw, I. S. Madjarov, X. Xie, R. Finkelstein, J. P. Covey, J. S. Cotler, D. K. Mark, H.-Y. Huang, A. Kale, H. Pichler, F. G. S. L. Brandão, S. Choi, and M. Endres, Preparing random states and benchmarking with many-body quantum chaos, Nature (London) **613**, 468 (2023).

[9] R. C. Farrell, M. Illa, A. N. Ciavarella, and M. J. Savage, Scalable circuits for preparing ground states on digital quantum computers: The Schwinger model vacuum on 100 qubits, PRX Quantum **5**, 020315 (2024).

[10] X. Mi *et al.*, Noise-resilient edge modes on a chain of superconducting qubits, Science **378**, 785 (2022).

[11] Daniel González-Cuadra, M. Hamdan, T. V. Zache, B. Braverman, M. Kornjača, A. Lukin, S. H. Cantú, F. Liu, S.-T. Wang, A. Keesling, M. D. Lukin, P. Zoller, and A. Bylinskii, Observation of string breaking on a (2 + 1)D Rydberg quantum simulator, Nature (London) **642**, 321 (2025).

[12] https://www.ibm.com/quantum/roadmap#content-block-simple-2.

[13] M. Kjaergaard, M. E. Schwartz, J. Braumüller, P. Krantz, J. I.-J. Wang, S. Gustavsson, and W. D. Oliver, Superconducting qubits: Current state of play, Annu. Rev. Condens. Matter Phys. **11**, 369 (2020).

[14] I. Siddiqi, Engineering high-coherence superconducting qubits, Nat. Rev. Mater. **6**, 875 (2021).

[15] K. R. Brown, J. Kim, and C. Monroe, Co-designing a scalable quantum computer with trapped atomic ions, npj Quantum Inf. **2**, 16034 (2016).

[16] T. M. Graham, E. Oh, and M. Saffman, Multiscale architecture for fast optical addressing and control of large-scale qubit arrays, Appl. Opt. **62**, 3242 (2023).

[17] C.-Y. Shih, S. Motlakunta, N. Kotibhaskar, M. Sajjan, R. Hablützel, and R. Islam, Reprogrammable and high-precision holographic optical addressing of trapped ions for scalable quantum control, npj Quantum Inf. **7**, 57 (2021).

[18] I. Pogorelov, T. Feldker, C. D. Marciniak, L. Postler, G. Jacob, O. Krieglsteiner, V. Podlesnic, M. Meth, V. Negnevitsky, M. Stadler, B. Höfer, C. Wächter, K. Lakhmanskiy, R. Blatt, P. Schindler, and T. Monz, Compact ion-trap quantum computing demonstrator, PRX Quantum **2**, 020343 (2021).

[19] G. Wang, W. Xu, C. Li, V. Vuletić, and P. Cappellaro, Individual-atom control in an array through phase modulation, Phys. Rev. Appl. **23**, 024072 (2025).

[20] F. Cesa and H. Pichler, Universal quantum computation in globally driven Rydberg atom arrays, Phys. Rev. Lett. **131**, 170601 (2023).

[21] B. Zhang, P. Peng, A. Paul, and J. D. Thompson, Scaled local gate controller for optically addressed qubits, Optica **11**, 227 (2024).

[22] D. Bluvstein *et al.*, A fault-tolerant neutral-atom architecture for universal quantum computation, Nature (London) **649**, 39 (2026).

[23] H. Zhou, C. Duckering, C. Zhao, D. Bluvstein, M. Cain, A. Kubica, S.-T. Wang, and M. D. Lukin, Resource analysis of low-overhead transversal architectures for reconfigurable atom arrays, in *Proceedings of the 52nd Annual International Symposium on Computer Architecture*, *SIGARCH'25* (ACM, Tokyo, 2025), p. 1432.

[24] A. Ransford *et al.*, A 98-qubit trapped-ion quantum computer with all-to-all connectivity, Nature (London) **655**, 81 (2026)

[25] M. Schlosser, S. Tichelmann, D. Schäffner, D. O. de Mello, M. Hambach, J. Schütz, and G. Birkl, Scalable multilayer architecture of assembled single-atom qubit arrays in a three-dimensional Talbot tweezer lattice, Phys. Rev. Lett. **130**, 180601 (2023).

[26] L. Pause, L. Sturm, M. Mittenbühler, S. Amann, T. Preuschoff, D. Schäffner, M. Schlosser, and G. Birkl, Supercharged two-dimensional tweezer array with more than 1000 atomic qubits, Optica **11**, 222 (2024).

[27] M. A. Norcia *et al.*, Iterative assembly of ^{171}Yb atom arrays with cavity-enhanced optical lattices, PRX Quantum **5**, 030316 (2024).

[28] F. Gyger, M. Ammenwerth, R. Tao, H. Timme, S. Snigirev, I. Bloch, and J. Zeiher, Continuous operation of large-scale atom arrays in optical lattices, Phys. Rev. Res. **6**, 033104 (2024).

[29] H. J. Manetsch, G. Nomura, E. Bataille, X. Lv, K. H. Leung, and M. Endres, A tweezer array with 6,100 highly coherent atomic qubits, Nature (London) **647**, 60 (2025).

[30] N.-C. Chiu, E. C. Trapp, J. Guo, M. H. Abobeih, L. M. Stewart, S. Hollerith, P. L. Stroganov, M. Kalinowski, A. A. Geim, S. J. Evered, S. H. Li, X. Lyu, L. M. Peters, D. Bluvstein, T. T. Wang, M. Greiner, V. Vuletić, and M. D. Lukin, Continuous operation of a coherent 3,000-qubit system, Nature (London) **646**, 1075 (2025).

[31] A. Binai-Motlagh, M. L. Day, N. Videnov, N. Greenberg, C. Senko, and R. Islam, A guided light system for agile individual addressing of Ba^+ qubits with 10^{-4} level intensity crosstalk, Quantum Sci. Technol. **8**, 045012 (2023).

[32] I. Christen, T. Propson, M. Sutula, H. Sattari, G. Choong, C. Panuski, A. Melville, J. Mallek, C. Brabec, S. Hamilton, P. B. Dixon, A. J. Menssen, D. Braje, A. H. Ghadimi, and D. Englund, An integrated photonic engine for programmable atomic control, Nat. Commun. **16**, 82 (2025).

[33] P. Schindler, D. Nigg, T. Monz, J. T. Barreiro, E. Martinez, S. X. Wang, S. Quint, M. F. Brandl, V. Nebendahl, C. F. Roos, M. Chwalla, M. Hennrich, and R. Blatt, A quantum information processor with trapped ions, New J. Phys. **15**, 123012 (2013).

[34] A. C. Lee, J. Smith, P. Richerme, B. Neyenhuis, P. W. Hess, J. Zhang, and C. Monroe, Engineering large Stark shifts for control of individual clock state qubits, Phys. Rev. A **94**, 042308 (2016).

[35] A. M. Polloreno, A. M. Rey, and J. J. Bollinger, Individual qubit addressing of rotating ion crystals in a Penning trap, Phys. Rev. Res. **4**, 033076 (2022).

[36] K. Barnes *et al.*, Assembly and coherent control of a register of nuclear spin qubits, Nat. Commun. **13**, 2779 (2022).

[37] A. L. Shaw, R. Finkelstein, R. B.-S. Tsai, P. Scholl, T. H. Yoon, J. Choi, and M. Endres, Multi-ensemble metrology by programming local rotations with atom movements, Nat. Phys. **20**, 195 (2024).

[38] H. Labuhn, S. Ravets, D. Barredo, L. Béguin, F. Nogrette, T. Lahaye, and A. Browaeys, Single-atom addressing in microtraps for quantum-state engineering using Rydberg atoms, Phys. Rev. A **90**, 023415 (2014).

[39] S. de Léséleuc, D. Barredo, V. Lienhard, A. Browaeys, and T. Lahaye, Optical control of the resonant dipole-dipole interaction between Rydberg atoms, Phys. Rev. Lett. **119**, 053202 (2017).

[40] W. J. Eckner, N. Darkwah Oppong, A. Cao, A. W. Young, W. R. Milner, J. M. Robinson, J. Ye, and A. M. Kaufman, Realizing spin squeezing with Rydberg interactions in an optical clock, Nature (London) **621**, 734 (2023).

[41] T. M. Graham *et al.*, Multi-qubit entanglement and algorithms on a neutral-atom quantum computer, Nature (London) **604**, 457 (2022).

[42] M. H. Levitt, Composite pulses, Prog. Nucl. Magn. Reson. Spectrosc. **18**, 61 (1986).

[43] J. T. Merrill and K. R. Brown, Progress in compensating pulse sequences for quantum computation, in *Quantum Information and Computation for Chemistry*, edited by S. A. Rice, A. R. Dinner, and S. Kais (John Wiley & Sons, Ltd., 2014), pp. 241–294.

[44] K. R. Brown, A. W. Harrow, and I. L. Chuang, Arbitrarily accurate composite pulse sequences, Phys. Rev. A **70**, 052318 (2004).

[45] D. Mc Hugh and J. Twamley, Sixth-order robust gates for quantum control, Phys. Rev. A **71**, 012327 (2005).

[46] H. K. Cummins and J. A. Jones, Use of composite rotations to correct systematic errors in NMR quantum computation, New J. Phys. **2**, 006 (2000).

[47] H. K. Cummins, G. Llewellyn, and J. A. Jones, Tackling systematic errors in quantum logic gates with composite rotations, Phys. Rev. A **67**, 042308 (2003).

[48] B. T. Torosov and N. V. Vitanov, High-fidelity error-resilient composite phase gates, Phys. Rev. A **90**, 012341 (2014).

[49] B. T. Torosov and N. V. Vitanov, Arbitrarily accurate twin composite π -pulse sequences, Phys. Rev. A **97**, 043408 (2018).

[50] S. Wimperis, Broadband, narrowband, and passband composite pulses for use in advanced NMR experiments, J. Magn. Reson. Ser. A **109**, 221 (1994).

[51] H. L. Gevorgyan and N. V. Vitanov, Ultrahigh-fidelity composite rotational quantum gates, Phys. Rev. A **104**, 012609 (2021).

[52] S. Kukita, H. Kiya, and Y. Kondo, General off-resonance-error-robust symmetric composite pulses with three elementary operations, Phys. Rev. A **106**, 042613 (2022).

[53] S. Kukita, H. Kiya, and Y. Kondo, Lower bound on operation time of composite quantum gates robust against pulse length error, J. Phys. A: Math. Theor. **56**, 485305 (2023).

[54] H. L. Gevorgyan and N. V. Vitanov, Ultrahigh-fidelity composite quantum phase gates, Phys. Rev. A **109**, 052625 (2024).

[55] C. Fromonteil, D. Bluvstein, and H. Pichler, Protocols for Rydberg entangling gates featuring robustness against quasistatic errors, PRX Quantum **4**, 020335 (2023).

[56] M. Bando, T. Ichikawa, Y. Kondo, and M. Nakahara, Concatenated composite pulses compensating simultaneous systematic errors, J. Phys. Soc. Jpn. **82**, 014004 (2013).

[57] J. Chen, D. Ding, C. Huang, and Q. Ye, Compiling arbitrary single-qubit gates via the phase shifts of microwave pulses, Phys. Rev. Res. **5**, L022031 (2023).

[58] G. H. Low, T. J. Yoder, and I. L. Chuang, Optimal arbitrarily accurate composite pulse sequences, Phys. Rev. A **89**, 022341 (2014).

[59] See Supplemental Material at https://link.aps.org/supplemental/10.1103/n2hz-8zy2 for detailed derivations and additional information on our numerical methods, which includes Refs. [67–69].

[60] T. Ichikawa, J. G. Filgueiras, M. Bando, Y. Kondo, M. Nakahara, and D. Suter, Construction of arbitrary robust one-qubit operations using planar geometry, Phys. Rev. A **90**, 052330 (2014).

[61] J. A. Jones, Designing short robust not gates for quantum computation, Phys. Rev. A **87**, 052317 (2013).

[62] S. Ma, G. Liu, P. Peng, B. Zhang, S. Jandura, J. Claes, A. P. Burgers, G. Pupillo, S. Puri, and J. D. Thompson, High-fidelity gates and mid-circuit erasure conversion in an atomic qubit, Nature (London) **622**, 279 (2023).

[63] M. Kang, W. C. Campbell, and K. R. Brown, Quantum error correction with metastable states of trapped ions using erasure conversion, PRX Quantum **4**, 020358 (2023).

[64] S. Jandura, J. D. Thompson, and G. Pupillo, Optimizing Rydberg gates for logical-qubit performance, PRX Quantum **4**, 020336 (2023).

[65] Z.-C. Shi, J.-T. Ding, Y.-H. Chen, J. Song, Y. Xia, X. Yi, and F. Nori, Supervised learning for robust quantum control in composite-pulse systems, Phys. Rev. Appl. **21**, 044012 (2024).

[66] D. C. McKay, C. J. Wood, S. Sheldon, J. M. Chow, and J. M. Gambetta, Efficient Z gates for quantum computing, Phys. Rev. A **96**, 022330 (2017).

[67] D. Suter and A. Pines, Recursive evaluation of interaction pictures, J. Magn. Reson. **75**, 509 (1987).

[68] S. Kukita, H. Kiya, and Y. Kondo, Short composite quantum gate robust against two common systematic errors, J. Phys. Soc. Jpn. **91**, 104001 (2022).

[69] N. H. Le, M. Cykiert, and E. Ginossar, Scalable and robust quantum computing on qubit arrays with fixed coupling, npj Quantum Inf. **9**, 1 (2023).